Neuroimage: Reports 6 (2026) 100327

Contents lists available at ScienceDirect

Neuroimage: Reports

journal homepage: www.sciencedirect.com/journal/neuroimage-reports

Functional brain connectivity in patients with *de novo* Parkinson's disease

Eliseo Picchi [a,1], Silvia Minosse [a,1], Noemi Pucci [a], Matteo Conti [b], Davide Mascioli [b], Alessandro Stefani [c], Francesco Garaci [a,c], Valentina Ferrazzoli [d], Valerio Da Ros [a], Tommaso Schirinzi [b], Francesca Di Giuliano [d,*]

[a] *Diagnostic Imaging Unit, University Hospital Tor Vergata, Viale Oxford 81, 00133, Rome, Italy*
[b] *Unit of Neurology, Department of Systems Medicine, Tor Vergata University of Rome, Italy*
[c] *San Raffaele Cassino, Via Gaetano di Biasio, 1, Cassino (Fr), 03043, Italy*
[d] *Neuroradiology Unit, Department of Biomedicine and Prevention, University of Rome Tor Vergata, Via Montpellier 1, 00133, Rome, Italy*

ARTICLE INFO

Keywords:
De novo Parkinson's disease
Resting-state fMRI (rs-fMRI)
Functional brain networks
Graph theory

ABSTRACT

Introduction: This study aims to identify early brain network changes in *de novo* Parkinson's disease (PD) using resting state-functional Magnetic Resonance Imaging (rs-fMRI), graph-theoretical analysis, and a functional brain network disruption index (k), applied here for the first time to *de novo* PD.
Materials and methods: The study enrolled untreated *de novo* PD patients and age- and sex-matched healthy controls. PD patients underwent comprehensive clinical assessments (MDS-UPDRS III, H&Y, MMSE, MoCA, NMSS). MRI data were acquired on a 3T system, including 3D T1-weighted MPRAGE and rs-fMRI. rs-fMRI data were pre-processed and analysed using graph theory.
Results: The study included 30 *de novo* PD patients and 30 healthy controls. While global network metrics did not differ significantly, local metrics revealed a reduced disruption index k in *de novo* PD patients. The disruption index k was negatively correlated with MMSE scores and demonstrated strong discriminatory power between PD patients and healthy controls based on clustering coefficient metrics. Significant differences in hub regions were found, as some disappeared in PD patients while others emerged compared to healthy controls.
Conclusions: This study provides evidence of widespread functional alterations in the local brain networks of *de novo* Parkinson's disease (PD) patients, suggesting early reorganization of brain connectivity. The disruption index (k) demonstrated the ability to detect early and subtle changes in functional brain networks in *de novo* Parkinson patients.
Significance: rs-fMRI can provide valuable insights into the early stages of PD pathophysiology helping to understand the complexity of PD.

1. Introduction

Parkinson's disease (PD) is a chronic neurodegenerative disorder, primarily characterized by the degeneration of dopaminergic neurons in the substantia nigra pars compacta (Poewe et al., 2017). However, it is now widely recognized as a multisystem condition, characterized by abnormal intraneuronal aggregates of α-synuclein, known as Lewy bodies, which can spread through a prion-like mechanism along neuronal networks and involve several cortical and subcortical regions (Borghammer, 2021; Braak et al., 2004). This network-based propagation underlies not only the classical motor features of PD, such as bradykinesia, rigidity, and tremor, but also the broad spectrum of non-motor symptoms, including anosmia, sleep disturbances, dysautonomia, and cognitive and affective changes, that may emerge years before the motor onset and define the prodromal phase of the disease (Horsager et al., 2019).

Clinically, the earliest symptomatic stage of PD is termed *de novo* PD, referring to patients not yet exposed to dopaminergic therapy. This stage provides a unique opportunity to study disease-related brain changes without the confounding effects of medication. Indeed,

* Corresponding author. Via Montpellier 1, 00133, Roma, Italy.
E-mail addresses: eliseo.picchi@uniroma2.eu (E. Picchi), silvia.minosse2@gmail.it (S. Minosse), noemi.pucci@students.uniroma2.eu (N. Pucci), matteoconti92@gmail.com (M. Conti), davidemascioli@outlook.it (D. Mascioli), stefani@uniroma2.it (A. Stefani), francesco.garaci@uniroma2.it (F. Garaci), valentinaferrazzoli@hotmail.it (V. Ferrazzoli), valerio.da.ros@uniroma2.it (V. Da Ros), t.schirinzi@yahoo.com (T. Schirinzi), francesca.di.giuliano@uniroma2.it (F. Di Giuliano).
[1] These authors contributed equally to this work.

https://doi.org/10.1016/j.ynirp.2026.100327
Received 24 September 2025; Received in revised form 13 December 2025; Accepted 5 February 2026
Available online 9 February 2026
2666-9560/© 2026 The Authors. Published by Elsevier Inc. This is an open access article under the CC BY-NC license (http://creativecommons.org/licenses/by-nc/4.0/).

neuropathological and neuroimaging evidence suggest that neurodegeneration in PD begins well before the appearance of motor symptoms, with axonal dysfunction and disruption of white matter integrity preceding neuronal cell death (Burke and O'Malley, 2013; O'Malley, 2010; Tagliaferro et al., 2015). Motor manifestations typically become evident only when the dopaminergic cell loss in the substantia nigra exceeds 50% (Hodaie et al., 2007), which underscores the need for reliable biomarkers capable of detecting PD during the prodromal or very early stages.

Although conventional Magnetic Resonance Imaging (MRI) is widely used in PD to rule out secondary parkinsonism related to structural lesions, it does not support early diagnosis of PD. In this context, advanced MRI techniques may detect subtle, non-structural changes in brain function, potentially enabling diagnosis even at early or prodromal stages, such as in *de novo* PD (Garaci et al., 2019; Minosse et al., 2020, 2019a; Minosse et al., 2021a).

Resting-state functional MRI (rs-fMRI) is a non-invasive MRI technique that measures intrinsic neuronal activity by assessing the levels of oxyhemoglobin and deoxyhemoglobin, which allow to explore brain connectivity. Although recent years have seen increasing interest in the application of rs-fMRI to investigate neural activation and functional organization in PD (Campbell et al., 2015; Chen et al., 2024; Göttlich et al., 2014; Li et al., 2018; Prodoehl et al., 2014; Tahmasian et al., 2015; Vo et al., 2017; Zhang et al., 2019), studies specifically examining rs-fMRI findings in *de novo* PD remain limited (Piramide et al., 2024).

The aim of this study is to investigate potential early reorganization of functional brain networks in de *novo* Parkinson's disease patients compared to healthy controls, by applying graph theory–based measures and the disruption index *k* to identify early biomarkers of the disease. In addition to conventional graph-theoretical metrics, we considered the disruption index *k*, a measure that quantifies how much the distribution of node-wise topological properties in patients deviates from that observed in healthy controls. Unlike global or local network metrics, which capture absolute properties of functional brain organization, the disruption index *k* reflects relative patterns of reorganization across the whole brain by comparing nodal values to a normative reference topology. This approach is particularly suited to detecting subtle disturbances in hub architecture and connectivity balance, which are expected to occur in the earliest stages of Parkinson's disease before large-scale changes in global efficiency or clustering become apparent. For these reasons, the disruption index *k* may provide a sensitive and complementary marker of early PD-related network alterations.

2. Materials and methods

2.1. Participants

This single-institution study was approved by the local institutional ethics committee [Ethical code and approval date: Progetto MNESYS "MUR PE0000000 Spoke6 WP4" R.S 133.23 (June 6, 2023)] and conducted in accordance with the Declaration of Helsinki; a written informed consent was obtained from all participants.

Patients diagnosed with *de novo* PD, according to the MDS clinical diagnostic criteria (Postuma et al., 2015), were eligible for inclusion in the study if they met the following criteria: 1) disease duration of less than 24 months; 2) no history of antiparkinsonian therapy; 3) no history of other neurological diseases, either past or concurrent, that could cause pathological alterations in the central nervous system (e.g., brain tumors, stroke, infections, etc.); 4) no cognitive impairment, defined as a Mini-Mental State Examination (MMSE) score greater than 25 (Folstein et al., 1975); 5) normal morphological MRI, without evidence of brain parenchymal lesions. A group of age- and sex-matched healthy controls with no history of neurological diseases was also enrolled.

PD patients underwent a comprehensive clinical evaluation, which included the MDS Unified Parkinson's Disease Rating Scale Part 3 (MDS-UPDRS III), and the Hoehn and Yahr scale (H&Y) to assess motor disturbances; the Mini-Mental State Examination (MMSE), adjusted for age and educational level, and the Montreal Cognitive Assessment (MoCA) to assess cognitive impairment; and the Non-Motor Symptoms Scale (NMSS).

2.2. Magnetic Resonance Imaging data acquisition

The MRI exam was performed within one week of the clinical assessments using a 3T superconductive scanner (Achieva d-Stream 3T, Philips Healthcare, Best, The Netherlands) equipped with a dedicated 32-channel sensitivity encoding head coil. The acquisition protocol included T1-weighted Multiplanar Progressively RApid Gradient-Echo (MPRAGE) images and rs-fMRI. MPRAGE images were acquired using the following parameters: field of view (FOV) 256 × 256 mm2, Repetition Time (TR) 6.5 ms, Echo Time (TE) 2.9 ms, flip angle 9° and voxel size 1 × 1 × 1 mm3. Rs-fMRI was performed using single-shot GE-EPI (Gradient-Echo Echo-Planar Imaging) with the following parameters: TR 2500 ms, TE 30 ms, flip angle 81°, FOV 240 × 240 mm2, slice number 45, voxel size 3x3x3 mm3 and 200 vol/subject. Additionally, 3D T2-weighted FLAIR (Fluid Attenuation Inversion Recovery) imaging and diffusion weighted imaging were acquired and evaluated by an expert neuroradiologist to exclude the presence of pathological findings.

2.3. Preprocessing of rs-fMRI data

rs-fMRI data preprocessing was carried out using FEAT-FMRI Expert Analysis Tool in FSL 6.0 (Jenkinson et al., 2012). After converting DICOM files to NIFTI data (outside of FSL), the first three volumes were discarded for scanner stabilization. Motion correction and slice timing correction were then applied using the MCFLIRT tool. Head motion was assessed using framewise displacement (FD) calculated with the *fsl_motion_outliers* tool, and a threshold of 0.5 mm was set to identify high-motion frames. Volumes exceeding this threshold would have been excluded from further analysis. Finally, preprocessed rs-fMRI data were nonlinearly coregistered to standard space using high-resolution T1-weighted MPRAGE images for subsequent time series extraction.

2.4. Structural brain network analyses

We analysed the functional brain network using graph theory analysis. The nodes of the brain network were defined by parcellating the whole brain into 116 regions using the AAL (The Automated Anatomical Labeling) atlas. The 116 regions included 90 in the cerebral cortex, 8 in the subcortical gray matter, and 18 in the cerebellum (Rolls et al., 2015). The network edges were defined as the partial correlation coefficients between the time series of each pair of nodes. Subsequently, a 116 x 116 connectivity matrix was used for each subject, binarized with a sparsity value of 10%, as commonly adopted in brain network literature (Minosse et al., 2019b; Minosse et al., 2021b; S. Minosse et al., 2021).

Graph-theoretical analyses were conducted using the Brain Connectivity Toolbox. We performed these analyses at both global and local levels to explore network alterations in *de novo* PD patients. The following local metrics were calculated for each subject: degree, betweenness centrality, local efficiency, clustering coefficient, and spectral measure of centrality. Furthermore, the global measures evaluated included global degree, global betweenness centrality, global efficiency, global clustering coefficient, transitivity, modularity, assortativity, and global spectral measure of centrality.

Node degree refers to the number of links connected to a given node. Node betweenness centrality represents the fraction of all shortest paths in the network that contain a given node. Nodes with high betweenness centrality participate in many shortest paths (Chalermsook et al., 2013). The clustering coefficient is the fraction of triangles around a node (equiv. the fraction of a node's neighbors that are neighbors of each other) (Kostić, 2018). Global efficiency is the average of the inverse shortest path length and is inversely related to the characteristic path

length. Local efficiency is the global efficiency computed on the neighborhood of the node and is related to the clustering coefficient (Rubinov and Sporns, 2010). Spectral measure of centrality is a self-referential measure of centrality: nodes have high eigenvector centrality if they connect to other nodes with high eigenvector centrality. The eigenvector centrality of node *i* is equivalent to the *ith* element in the eigenvector corresponding to the largest eigenvalue of the adjacency matrix (Newman, 2010). Transitivity is the ratio of 'triangles to triplets' in the network (Humphries and Gurney, 2008). Modularity is a statistic that quantifies the degree to which the network can be subdivided into clearly delineated groups (Reichardt and Bornholdt, 2006). The assortativity coefficient is a correlation coefficient between the degrees of all nodes on two opposite ends of a link. A positive assortativity coefficient indicates that nodes tend to link to other nodes with the same or similar degree (Newman, 2002). Global degree is the mean degree of all nodes within brain network. Global between centrality is defined as the mean between centrality of all the nodes in the brain network. Global clustering coefficient is the mean clustering coefficient of all nodes in the brain network. Global Spectral measure of centrality is the mean spectral measure of centrality of all nodes in the brain network.

These analyses were implemented using the BCT (Brain Connectivity Toolbox) toolbox (Rubinov and Sporns, 2010). To examine group differences in local measures (degree, betweenness centrality, local efficiency, clustering coefficient, and spectral measure of centrality), we employed the disruption index *k*, which quantifies the level of global reorganization of a specific topological network property across the whole brain. The slope of the linear regression, either at a single subject level or at a group of subjects' level, was used to obtain the disruption index *k* for each local measure as described in the literature (Minosse et al., 2019b; Silvia Minosse et al., 2021b; S. Minosse et al., 2021). A disruption index *k* equal to zero ($k = 0$) for a particular network measure indicates that, on average, that node-wise network measure for *de novo* PD patients is statistically similar to the mean of the same node measure across healthy control subjects. If this condition is not met, it suggests reorganization of the brain's topological network properties as represented by that metric. The disruption index *k* summarizes changes in local theoretical metrics into a single value.

Finally, we examined group differences in the so-called hub regions. A region was classified as a hub for each subject if any of the local network measures was 1.5 times greater than the mean of that same measure across the entire brain (S. Minosse et al., 2021).

2.5. Statistical analysis

The nonparametric Wilcoxon rank sum test for independent samples was performed to compare the graph-theoretical analysis (including both global and local measures) and disruption index *k* between *de novo* PD patients and healthy control subjects. Effect sizes for these comparisons were calculated using the rank-biserial correlation, which is appropriate for non-parametric data. The Fisher's exact test was applied to evaluate group differences in the presence or absence of hubs.

The relationship between clinical variables and functional brain measures (including global and local graph-theoretical measures and disruption index *k*) was assessed using the Spearman's Rho correlation test, while controlling for the effects of age and gender. Spearman's Rho is reported as the effect size for each correlation.

To exclude false positive results (In the case of local measures) under multiple testing, the false discovery rate (FDR) procedure was applied, choosing an FDR of 0.05.

Receiver operating characteristic (ROC) curves were implemented to determine the optimum thresholds for the most significant parameters, based on the Youden's index (which maximizes both sensitivity and specificity) (Fluss et al., 2005).

Sensitivity, specificity, positive predicted value (PPV) and negative predicted value (NPV) were calculated. The Area Under the Curve (AUC), along with sensitivity and specificity, is reported as the standard measure of effect size for diagnostic accuracy. A p-value <0.05 was considered statistically significant.

Data analyses were performed using MATLAB version 9.90, release 2020b (MathWorks, Natick, MA, USA).

3. Results

A total of 65 subjects were initially selected for this study. *De novo* PD patients were monitored for a minimum of 2 years to confirm the diagnosis. Accordingly, three patients were excluded due to misdiagnosis, and two subjects were excluded because of significant motion artifacts in MPRAGE imaging.

The final population consisted of 30 *de novo* PD patients and 30 healthy control subjects.

The *de novo* PD patient group included 22 men and 8 women, with an average age of 60 years (range 32–76 years). The healthy control group, matched by age (p-value = 0.73, Mann Whitney *U* test) and gender (p-value = 0.10 Chi-square test), consisted of 16 men and 14 women, with an average age of 57 years (range 28–79). Cognitive scores (MoCA/MMSE) were not collected for the healthy control subjects. Demographic, clinical, and biochemical data of *de novo* PD patients and healthy control subjects are summarized in Table 1.

Across all subjects, FD ranged between 0 and 0.19 mm. No frames exceeded the 0.5 mm threshold, and therefore no volumes were removed. Mean absolute displacement ranged from 0.17 to 1.09 mm, and mean relative displacement (frame-to-frame) ranged from 0.04 to 0.15 mm. All participants retained the 197 vol (after removal of the first three volumes to allow for scanner stabilization), and no subjects were excluded due to excessive motion.

The effect sizes (rank-biserial correlation) of disruption indices at the single-subject level, calculated from degree, betweenness centrality, local efficiency, clustering coefficient, and spectral measure of centrality, ranged from 0.35 to 0.51, corresponding to medium to large effects. Specifically, rank-biserial correlations were 0.357 for degree, 0.385 for betweenness centrality, 0.462 for local efficiency, 0.514 for clustering coefficient, and 0.355 for the spectral measure of centrality.

No statistically significant differences in global and local theoretical metrics between *de novo* PD patients and healthy control subjects. However, when evaluating the disruption index *k*, statistically significant differences were found at both single subject and group of subjects in all local metrics, as reported in Figs. 1 and 2 respectively. Decreased and negative disruption index k values for *de novo* PD patients, compared to healthy control subjects, were observed in all local metrics.

Regions classified as hubs that were present or absent in *de novo* PD patients but not in healthy controls are illustrated in Fig. 3. The right inferior frontal gyrus (triangular part) was classified as a local efficiency hub in *de novo* PD patients but not in healthy control subjects (p =

Table 1
Demographic, clinical, and biochemical data of the study population.

	De novo PD patients	Healthy control subjects	p-value
Subject number	30	30	
Age (years and range)	60 (32-76)	57 (28-79)	0.73[a]
Sex (male/female)	22/8	16/14	0.10[b]
BMI (kg/m^2)	21.50 ± 2.12	Not collected	
MMSE	28.63 ± 1.71	Not collected	
MoCA	26.08 ± 2.41	Not collected	
H&Y	1.77 ± 0.53	-	
MDS-UPDRS III	27.43 ± 11.47	-	
NMSS	31.00 ± 25.90	-	

Abbreviations: PD, Parkinson's disease; BMI, body mass index; MMSE, Mini-Mental State Examination; MoCA, Montreal Cognitive Assessment; H&Y, Hoehn and Yahr scale; MDS-UPDRS III, Movement Disorder Society Unified Parkinson's Disease Rating Scale; NMSS, Non-Motor Symptoms Scale.

[a] Mann Whitney *U* test.

[b] Chi square test.

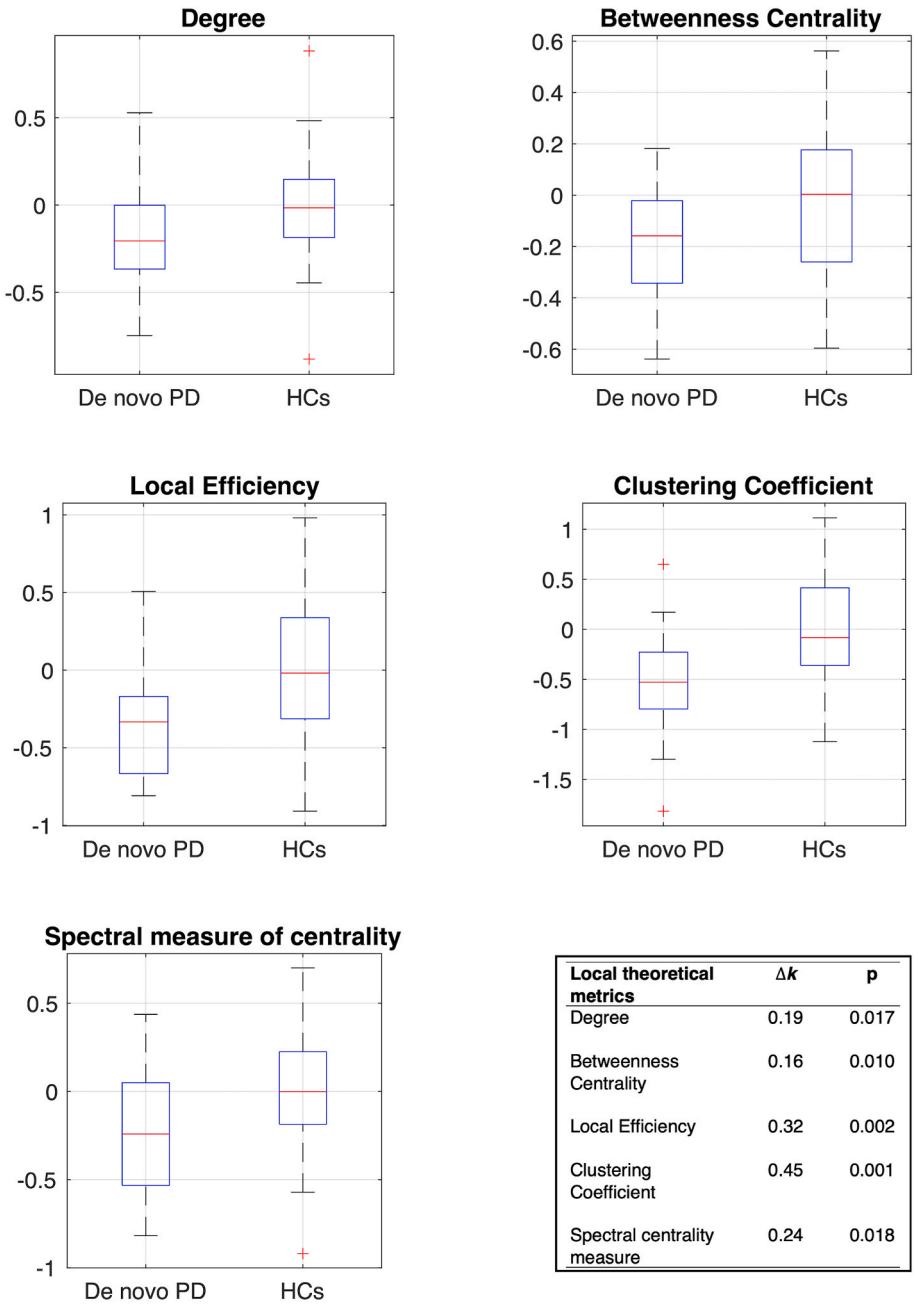

Local theoretical metrics	Δ*k*	p
Degree	0.19	0.017
Betweenness Centrality	0.16	0.010
Local Efficiency	0.32	0.002
Clustering Coefficient	0.45	0.001
Spectral centrality measure	0.24	0.018

Fig. 1. Box and whisker plots of disruption indices (at the single subject level) calculated from degree, betweenness centrality, local efficiency, clustering coefficient, and spectral measure of centrality in the two groups: *de novo* PD patients (*de novo* PD) and healthy control subjects (HCs). * = $p < 0.05$.
Bottom right: Δk, difference between the median values of subject-wise disruption indices, representing the magnitude of the group effect, with p-values resulting from Mann–Whitney-U-tests.

0.043), while the right lobule IX of cerebellar hemisphere (p = 0.011) exhibited the opposite pattern. The right calcarine fissure and surrounding cortex were classified as a cluster coefficient hub in *de novo* PD patients but not in healthy control subjects (p = 0.022). The right superior frontal gyrus, medial, was classified as a local efficiency hub in healthy control subjects but not in *de novo* PD patients (p = 0.040), The right gyrus rectus was classified as a hub for local efficiency and cluster coefficient in healthy controls but not in *de novo* PD patients (p = 0.043 and 0.026, respectively). The right thalamus, the left crus II of cerebellar hemisphere, and the lobule I, II of vermis were classified cluster coefficient hubs in healthy controls but not in *de novo* PD patients (p = 0.031, p = 0.011 and p = 0.012, respectively). Finally, the lobule III of vermis was classified as a betweenness centrality hub in healthy control subjects but not in *de novo* PD patients (p = 0.031).

The relationships between clinical variables and global functional brain measures were not statistically significant after FDR correction. However, the disruption index computed from the spectral measure of centrality was strongly and negatively correlated with MMSE (Rho = −0.64, p-value after FDR correction = 0.044). Significant correlations between clinical variables and local functional brain measures were identified in several regions, with the corresponding correlation coefficients presented in Table 2. Areas under the ROC curves (AUCs) for the global metrics and disruption index k are reported in Table 3, with the optimal cutoff values and the corresponding sensitivity and specificity. The disruption index k based on the clustering coefficient metrics demonstrated the best discriminative powers for differentiating *de novo*

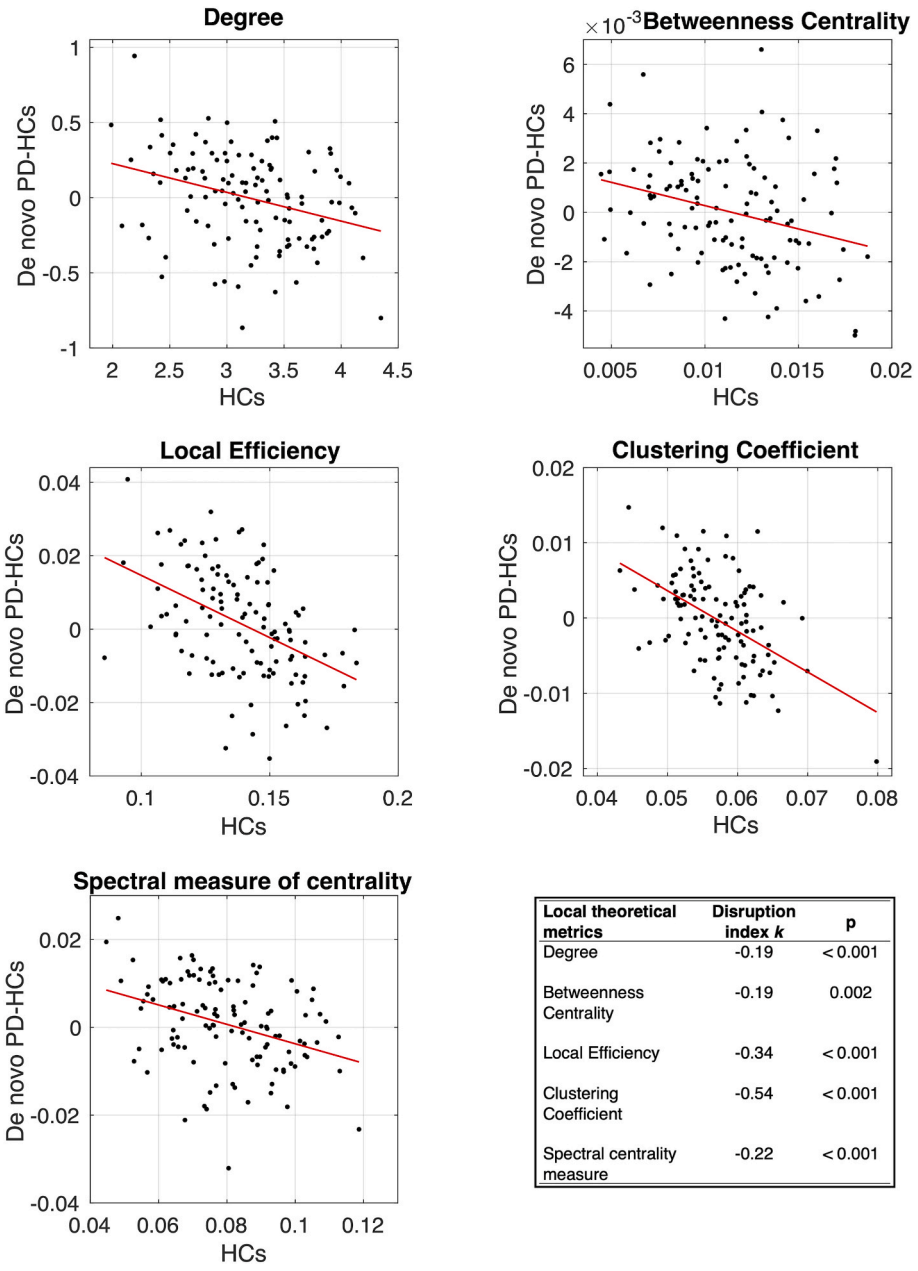

Local theoretical metrics	Disruption index *k*	p
Degree	-0.19	< 0.001
Betweenness Centrality	-0.19	0.002
Local Efficiency	-0.34	< 0.001
Clustering Coefficient	-0.54	< 0.001
Spectral centrality measure	-0.22	< 0.001

Fig. 2. Computation of the disruption index *k* (group of subjects' level) for separate network measures. The y-axis represents the difference between the mean value of the network measures (i = degree, betweenness centrality, local efficiency, clustering coefficient, and spectral measure of centrality) for the single node in *de novo* PD patient and the mean value of the network measure (i) for each node in healthy control subjects. This latter quantity is also reported in the x-axis (mean value of the network measures (i) of each node obtained in the healthy control subjects). The disruption index *k* is the slope of the linear regression.
Bottom right: disruption index *k* obtained from the slope of the linear regression, representing the magnitude of the systematic group difference, and the corresponding p-value.

PD patients and healthy control subjects (Fig. 4).

Finally, Table 4 presents the top 10 AUC values achieved when individual local graph-theoretical metrics were used as independent variables, which demonstrated only moderate discriminatory ability (highest AUC = 0.71).

4. Discussion

The present study examines the utility of rs-fMRI in individuals diagnosed with *de novo* PD within the past two years and who have not yet received pharmacological treatment. A graph-theoretic analysis was performed to assess the functional connectivity of neuronal networks using both local and global measures, alongside a developed network disruption index k, to characterize early network alterations.

Even though no statistically significant differences were observed in the global graph-theoretic measures between *de novo* PD patients and healthy controls, the disruption index k was significantly lower across all local network measures in the *de novo* PD patients. This finding indicates that early and widespread brain network reorganization can be detected already in the initial stages of the disease using disruption index k. The extensive impairment of the local graph-theoretic measures revealed by our analysis appears consistent with the disease phase analysed (*de novo* PD). In fact, in *de novo* PD patients, local metrics showed significant reductions in the disruption index, particularly for the clustering coefficient and local efficiency, suggest early impairment of local functional integration, especially in regions involved in motor and cognitive

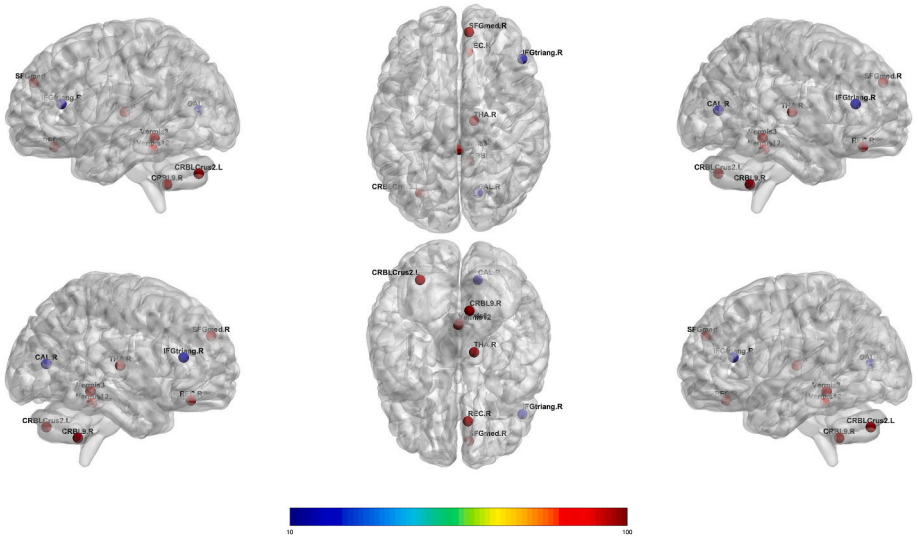

Fig. 3. Regions classified as hubs in *de novo* PD patients and healthy control subjects. Blue regions represent hubs present only in *de novo* PD patients but not in healthy control subjects. Red regions represent hubs found only in healthy controls but not in PD patients. IFGtriang.R, right inferior frontal gyrus; SFGmed.R, right superior frontal gyrus, medial; REC.R, right gyrus rectus; CAL.R, right calcarine fissure and surrounding cortex; THA.R, right thalamus; CRBLCrus2.L, left crus II of cerebellar hemisphere; CRBL9.R, right lobule IX of cerebellar hemisphere; Vermis12, lobule I, II of vermis; Vermis3, lobule III of vermis.

Table 2
Results Spearman's Rho correlation test between clinical variables and local functional brain measures. $p < 0.05$ after false discovery rate correction.

Regions (AAL atlas)	Network measures	Clinical parameters	Rho	p-value
Right anterior cingulate and paracingulate gyri	Clustering Coefficient	MDS-UPDRS III	0.62	0.021
Left putamen	Clustering Coefficient	MDS-UPDRS III	0.63	0.014
Left Inferior temporal gyrus	Local Efficiency	H&Y	0.58	0.042
Left Inferior temporal gyrus	Clustering Coefficient	H&Y	0.62	0.028

Abbreviations: MDS-UPDRS III, Movement Disorder Society Unified Parkinson's Disease Rating Scale; H&Y, Hoehn and Yahr scale; AAL atlas: Automated Anatomical Labeling atlas.

Table 3
AUCs for the global metrics and disruption index *k* as predictors for *de novo* PD patients, with the optimal cutoff values and the corresponding Sensitivity and Specificity.

Network measures	AUC	Sens (%)	Spec (%)	PPV (%)	NPV (%)
k Clustering Coefficient	0.757	77	71	72	76
k Local Efficiency	0.731	73	71	71	73
k Betweenness Centrality	0.692	67	71	69	69
k Degree	0.678	73	58	63	69
k Spectral measure of centrality	0.677	80	55	63	74
Global Clustering Coefficient	0.549	60	58	58	60
Global Efficiency	0.542	63	52	56	59
Transitivity	0.533	63	52	56	59
Global Degree	0.532	70	45	55	61
Modularity	0.459	73	39	54	60
Assortativity	0.451	63	35	49	50
Global Betweenness Centrality	0.447	50	55	52	53
Global Spectral measure of centrality	0.444	60	45	51	54

Abbreviations: AUC, area under the receiver operating characteristic curve; Sens., sensitivity; Spec., specificity, PPV, positive predicted value; NPV, negative predicted value.

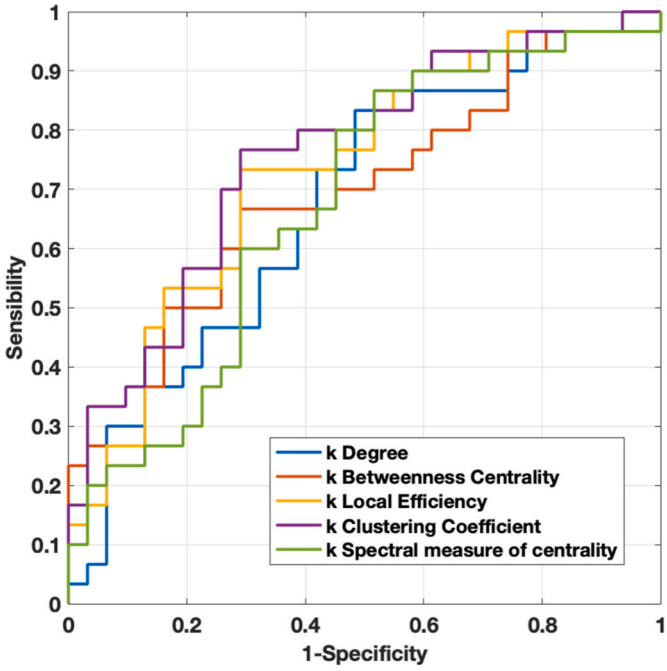

Fig. 4. ROC curves calculated using the disruption index *k (*derived from degree, betweenness centrality, local efficiency, clustering coefficient, and spectral measure of centrality) to discriminate *de novo* PD patients and healthy control subjects.

processing. Moreover, since the clustering coefficient and local efficiency respectively reflect local network segregation and integration among neighbour nodes, the reduction of their disruption indices k suggests early impairments in local functional integration and resilience, particularly in brain areas involved in motor and cognitive processing. Interestingly clustering coefficient and local efficiency showed significant correlations with MDS-UPDRS III and H&Y scales in the right anterior cingulate and paracingulate gyri, the left putamen, and the left inferior temporal gyrus. Although a strong and expected correlation was observed in the left putamen - related to bradykinesia and rigidity due to

Table 4
AUCs for the local metrics as predictors for *de novo* PD patients, with the optimal cutoff values and the corresponding Sensitivity and Specificity.

Regions	Network measures	AUC	Sens (%)	Spec (%)	PPV (%)	NPV (%)
Right Middle occipital gyrus	Clustering Coefficient	0.708	63	81	76	69
Right Lobule IX of cerebellar hemisphere	Spectral measure of centrality	0.706	63	77	73	69
Right Lobule IX of cerebellar hemisphere	Degree	0.701	70	61	64	68
Right Lobule IX of cerebellar hemisphere	Betweenness Centrality	0.684	77	61	66	73
Left Angular gyrus	Clustering Coefficient	0.654	67	68	67	68
Right Postcentral gyrus	Clustering Coefficient	0.652	73	65	67	71
Right Lobule IX of cerebellar hemisphere	Local Efficiency	0.649	63	65	63	65
Left Lenticular nucleus, Pallidum	Spectral measure of centrality	0.646	73	68	69	72
Left Gyrus rectus	Degree	0.641	63	65	63	65
Lobule III of vermis	Betweenness Centrality	0.637	57	68	63	62

Abbreviations: AUC, area under the receiver operating characteristic curve; Sens., sensitivity; Spec., specificity, PPV, positive predicted value; NPV, negative predicted value.

dopaminergic degeneration, which aligns with the putamen's role as a key region for spontaneous motor initiation - the correlations in the right anterior cingulate and paracingulate gyri appear to be more subtle. The right anterior cingulate gyrus and the paracingulate gyrus are known to support a range of cognitive, emotional, and social functions. In particular, the anterior cingulate gyrus, a key component of the limbic system, is involved in emotion processing, attentional control, and memory formation, playing a crucial role in integrating social information. Reductions in functional connectivity and alterations in subcortical white matter in this region have been associated with decreased motivation, a core mechanism underlying the development of apathy (Apps et al., 2016; Drevets et al., 2008; Hadland et al., 2003; Makris et al., 2015; Onoda and Yamaguchi, 2015).

The paracingulate gyrus, on the other hand, is implicated in cognitive empathy, moral reasoning, and the integration of cognitive–emotional processes, as well as in self-awareness. Alterations in this region have been linked to impairments in cognitive–attentional control, emotional and motivational regulation, memory, and sleep—features that may emerge in the early stages of the disease and often precede motor symptoms (Gennari et al., 2018; Karagoz et al., 2025; Wang et al., 2025).

These findings suggest that the disruption index k may be particularly useful in distinguishing *de novo* PD patients from healthy controls.

Supporting our observations, Luo et al. reported a reduction in local efficiency and local clustering coefficient within mesolimbic-striatal and corticostriatal circuits in drug naive PD patients (Luo et al., 2014). Similar to our study, the authors investigated patients in the early stage of PD who had not yet been treated with antiparkinsonian drugs, to exclude the potential confounding effects of prolonged drug use on the functional integration of neural networks.

A particularly intriguing finding is the pronounced negative correlation between the disruption index, derived from the spectral measure of centrality, and MMSE scores, suggesting a potential link between network organization and cognitive performance. The present result is particularly intriguing, as it suggests that network reorganization - captured by the index k - may already be detectable in the early stages of the disease. In particular, spectral measure of centrality indicates alterations in the structural importance of specific nodes within the network. A lower disruption index reflects a more synchronized, organized, and potentially more efficient network configuration, which could support better cognitive performance. This interpretation aligns with the observed association between lower k values and higher MMSE scores, suggesting that preserved network organization may contribute to maintained global cognition.

Moreover, our results provide also new insights into functional alterations in the brains of patients with *de novo* PD, extending existing knowledge on the reconfiguration of functional brain networks related to this disease. This widespread whole-brain functional reorganization is reflected in network disruption, with specific hubs showing functional rearrangement compared to healthy controls. Several supra- and infratentorial hub regions implicated in complex motor networks, consistently observed in healthy controls, were notably absent in *de novo* PD patients. These results support underline previous rs-fMRI findings reporting decreased functional connectivity within cerebello-thalamo-cortical circuits during the early stages of PD which have been associated with alterations in sensory-motor networks observed at early disease stages in particular at thalamic region (Agosta et al., 2014; H. C. Baggio et al., 2014; Esposito et al., 2013; Fang et al., 2017; Planetta et al., 2013; Owens-Walton et al., 2019; Wang et al., 2025). An interesting finding concerns the thalamus, which may undergo network reorganization as early as the initial stages of the disease, potentially leading to reduced cortical activation due to deafferentation mechanisms (Albin et al., 1989). Additionally, as part of the limbic system, the thalamus plays a crucial role in relaying sensory and motor information to the cerebral cortex and in regulating emotional and cognitive process (Lanciego et al., 2012; Moustafa et al., 2017). A reduction in local measures was also found in the cerebellum in *de novo* PD patients compared to healthy controls, in contrast to other studies which have reported hypercompensatory hyperactivation of the cerebellum in PD patients undergoing treatment. This discrepancy may indicate that cerebellar function in PD is mediated by both pathogenic and compensatory processes, depending on dopaminergic treatment or clinical symptoms (Mirdamadi, 2016).

Although its precise function remains unclear, the gyrus rectus is considered part of the orbitofrontal cortex and has been implicated in higher-order cognitive processes, which are part of the non-motor symptom spectrum and may emerge as early as the initial stages of PD (Bhattacharjee, 2018; Li et al., 2021; Pfeiffer et al., 2014; Rudebeck and Rich, 2018).

Conversely, the right inferior frontal gyrus and the calcarine gyrus were identified as network hubs exclusively in *de novo* PD patients compared to healthy controls. This finding may suggest an overactivation of these areas, which include regions of the visual cortex, potentially correlating with the visual hallucinations experienced by some patients in the later stages of the disease (de Schipper et al., 2018; Hu et al., 2015). These findings contrast with previous studies that reported reduced activation of visual areas, particularly the occipital cortex (Fang et al., 2017) as well as decreased connectivity in the occipital lobe and calcarine region in PD patients compared to healthy controls (Göttlich et al., 2013). However, it is important to note that all participants in these studies were undergoing treatment with anti-Parkinson medication.

The present findings do not align with those of previous studies, which demonstrated a significant reduction in global measures but no significant differences in local brain network measures in individuals with early- and intermediate-stage PD who had received antiparkinsonian drug therapy compared to controls (H. Baggio et al., 2014; Sang et al., 2015; Skidmore et al., 2011). This discrepancy may suggest that treatment with antiparkinsonian drugs affects the global efficiency of the brain network, which has not yet been significantly compromised

in the *de novo* PD patients not exposed to therapies.

In conclusion, our study demonstrated widespread functional alterations in *de novo* PD patients, suggesting a reorganization of brain networks already during the early stages of the disease. To the best of our knowledge, this is the first study to identify and characterize a reorganization of brain networks using the "disruption index" in *de novo* PD patients.

Our results go beyond what was recently reported, suggesting that altered functional connectivity of brain networks may serve as a potential neuroimaging biomarker for PD even in its early stages (Zhou et al., 2023).

The present study has several limitations. First, the relatively small sample size (n = 30 per group) may limit the generalizability of the findings. Nevertheless, the effect sizes (rank-biserial correlation) of the disruption indices *k* support the reliability of the observed differences between de *novo* PD patients and healthy controls. Second, given the limited sample, ROC analyses were not validated using cross-validation or bootstrap resampling; therefore, the reported AUC values may overestimate the true generalizability of the findings and should be interpreted as exploratory. Finally, future multicenter studies with larger patient populations and longer-term follow-up are needed to further assess the potential of brain network disruption indices *k* as sensitive biomarkers for diagnosis, disease progression, and brain involvement in de *novo* PD patients, as well as to clarify the direction of potential causal relationships between clinical features and brain functional alterations in this disorder.

CRediT authorship contribution statement

Eliseo Picchi: Writing – original draft, Resources, Methodology, Data curation. **Silvia Minosse:** Methodology, Formal analysis, Data curation. **Noemi Pucci:** Writing – original draft, Investigation. **Matteo Conti:** Writing – original draft, Investigation. **Davide Mascioli:** Supervision, Investigation. **Alessandro Stefani:** Supervision, Conceptualization. **Francesco Garaci:** Supervision, Conceptualization. **Valentina Ferrazzoli:** Writing – original draft, Investigation. **Valerio Da Ros:** Validation, Supervision. **Tommaso Schirinzi:** Investigation, Conceptualization. **Francesca Di Giuliano:** Writing – review & editing, Project administration, Conceptualization.

Informed consent statement

Informed consent was obtained from all subjects involved in the study.

Funding

This research is supported by #NEXTGENERATIONEU (NGEU) and funded by the Ministry of University and Research (MUR), National Recovery and Resilience Plan (NRRP), project MNESYS (PE0000006) - A Multiscale integrated approach to the study of the nervous system in health and disease (DN. 1553 October 11, 2022).

Declaration of competing interest

The authors declare the following financial interests/personal relationships which may be considered as potential competing interests: Francesca Di Giuliano reports financial support was provided by Next Generation. If there are other authors, they declare that they have no known competing financial interests or personal relationships that could have appeared to influence the work reported in this paper.

Data availability

Data will be made available on request.

References

Agosta, F., Caso, F., Stankovic, I., Inuggi, A., Petrovic, I., Svetel, M., Kostic, V.S., Filippi, M., 2014. Cortico-striatal-thalamic network functional connectivity in hemiparkinsonism. Neurobiol. Aging 35, 2592–2602. https://doi.org/10.1016/j.neurobiolaging.2014.05.032.

Albin, R.L., Young, A.B., Penney, J.B., 1989. The functional anatomy of basal ganglia disorders. Trends Neurosci. 12, 366–375. https://doi.org/10.1016/0166-2236(89)90074-X.

Apps, M.A.J., Rushworth, M.F.S., Chang, S.W.C., 2016. The anterior cingulate gyrus and social cognition: tracking the motivation of others. Neuron 90, 692–707. https://doi.org/10.1016/j.neuron.2016.04.018.

Baggio, H., Sala-Llonch, R., Segura, B., Marti, M., Valldeoriola, F., Compta, Y., Tolosa, E., Junqué, C., 2014. Functional brain networks and cognitive deficits in Parkinson's disease. Hum. Brain Mapp. 35, 4620–4634. https://doi.org/10.1002/hbm.22499.

Bhattacharjee, S., 2018. Impulse control disorders in Parkinson's disease: review of pathophysiology, epidemiology, clinical features, management, and future challenges. Neurol. India 66, 967–975. https://doi.org/10.4103/0028-3886.237019.

Borghammer, P., 2021. The α-Synuclein origin and connectome model (SOC model) of parkinson's disease: explaining motor asymmetry, non-motor phenotypes, and cognitive decline. J. Parkinsons Dis. https://doi.org/10.3233/JPD-202481.

Braak, H., Ghebremedhin, E., Rüb, U., Bratzke, H., Del Tredici, K., 2004. Stages in the development of Parkinson's disease-related pathology. Cell Tissue Res. 318, 121–134. https://doi.org/10.1007/s00441-004-0956-9.

Burke, R.E., O'Malley, K., 2013. Axon degeneration in Parkinson's disease. Exp. Neurol. https://doi.org/10.1016/j.expneurol.2012.01.011.

Campbell, M.C., Koller, J.M., Snyder, A.Z., Buddhala, C., Kotzbauer, P.T., Perlmutter, J. S., 2015. CSF proteins and resting-state functional connectivity in Parkinson disease. Neurology 84. https://doi.org/10.1212/WNL.0000000000001681.

Chalermsook, P., Kintali, S., Lipton, R.J., Nanongkai, D., 2013. Graph Pricing Problem on Bounded Treewidth, Bounded Genus and k-Partite Graphs. Chicago J. Theor. Comput. Sci. 13, 1–19. https://doi.org/10.4086/cjtcs.2013.013.

Chen, Z., He, C., Zhang, P., Cai, X., Li, X., Huang, W., Huang, S., Cai, M., Wang, L., Zhan, P., Zhang, Y., 2024. Brain network centrality and connectivity are associated with clinical subtypes and disease progression in Parkinson's disease. Brain Imaging Behav 18. https://doi.org/10.1007/s11682-024-00862-1.

de Schipper, L.J., Hafkemeijer, A., van der Grond, J., Marinus, J., Henselmans, J.M.L., van Hilten, J.J., 2018. Altered whole-brain and network-based functional connectivity in parkinson's disease. Front. Neurol. 9. https://doi.org/10.3389/fneur.2018.00419.

Drevets, W.C., Savitz, J., Trimble, M., 2008. The subgenual anterior cingulate cortex in mood disorders. CNS Spectr. 13, 663–681. https://doi.org/10.1017/S1092852900013754.

Esposito, F., Tessitore, A., Giordano, A., De Micco, R., Paccone, A., Conforti, R., Pignataro, G., Annunziato, L., Tedeschi, G., 2013. Rhythm-specific modulation of the sensorimotor network in drug-naïve patients with Parkinson's disease by levodopa. Brain 136, 710–725. https://doi.org/10.1093/brain/awt007.

Fang, J., Chen, H., Cao, Z., Jiang, Y., Ma, L., Ma, H., Feng, T., 2017. Impaired brain network architecture in newly diagnosed Parkinson's disease based on graph theoretical analysis. Neurosci. Lett. 657, 151–158. https://doi.org/10.1016/j.neulet.2017.08.002.

Fluss, R., Faraggi, D., Reiser, B., 2005. Estimation of the youden index and its associated cutoff point. Biom. J. 47, 458–472. https://doi.org/10.1002/bimj.200410135.

Folstein, M.F., Folstein, S.E., McHugh, P.R., 1975. "Mini-mental state." A practical method for grading the cognitive state of patients for the clinician. J. Psychiatr. Res. 12. https://doi.org/10.1016/0022-3956(75)90026-6.

Garaci, F., Picchi, E., Di Giuliano, F., Lanzafame, S., Minosse, S., Manenti, G., Pistolese, C. A., Sarmati, L., Teti, E., Andreoni, M., Floris, R., Toschi, N., 2019. Cerebral multishell diffusion imaging parameters are associated with blood biomarkers of disease severity in HIV infection. J. Neuroimaging 29, 771–778. https://doi.org/10.1111/jon.12655.

Gennari, S.P., Millman, R.E., Hymers, M., Mattys, S.L., 2018. Anterior paracingulate and cingulate cortex mediates the effects of cognitive load on speech sound discrimination. Neuroimage 178, 735–743. https://doi.org/10.1016/j.neuroimage.2018.06.035.

Göttlich, M., Jandl, N.M., Wojak, J.F., Sprenger, A., Der Gablentz, J. Von, Münte, T.F., Krämer, U.M., Helmchen, C., 2014. Altered resting-state functional connectivity in patients with chronic bilateral vestibular failure. Neuroimage, Clin. 4. https://doi.org/10.1016/j.nicl.2014.03.003.

Göttlich, M., Münte, T.F., Heldmann, M., Kasten, M., Hagenah, J., Krämer, U.M., 2013. Altered resting state brain networks in parkinson's disease. PLoS One 8, e77336. https://doi.org/10.1371/journal.pone.0077336.

Hadland, K.A., Rushworth, M.F.S., Gaffan, D., Passingham, R.E., 2003. The effect of cingulate lesions on social behaviour and emotion. Neuropsychologia 41, 919–931. https://doi.org/10.1016/S0028-3932(02)00325-1.

Hodaie, M., Neimat, J.S., Lozano, A.M., 2007. The dopaminergic nigrostriatal system and Parkinson's disease: molecular events in development, disease, and cell death, and new therapeutic strategies. Neurosurgery. https://doi.org/10.1227/01.NEU.0000249209.11967.CB.

Horsager, J., Knudsen, K., Andersen, K., Skjaerbaek, C., Fedorova, T., Geday, J., Kraft, J., Bech, E., Danielsen, E., Moller, M., Pavese, N., Brooks, D., Borghammer, P., 2019. "brain-first" vs. "body-first" Parkinson's disease is determined by RBD-status - a multi-modality imaging study. Mov. Disord. 34.

Hu, X., Song, X., Yuan, Y., Li, E., Liu, J., Liu, W., Liu, Y., 2015. Abnormal functional connectivity of the amygdala is associated with depression in Parkinson's disease. Mov. Disord. 30, 238–244. https://doi.org/10.1002/MDS.26087.

Humphries, M.D., Gurney, K., 2008. Network "small-world-ness": a quantitative method for determining canonical network equivalence. PLoS One 3. https://doi.org/10.1371/journal.pone.0002051.

Jenkinson, M., Beckmann, C.F., Behrens, T.E.J., Woolrich, M.W., Smith, S.M., 2012. FSL - Review. Neuroimage. https://doi.org/10.1016/j.neuroimage.2011.09.015.

Karagoz, B., Temel, Z., Ertan, G., Velioglu, H.A., Salar, A.B., Sakul, B.U., Hanoglu, L., 2025. The relationship between paracingulate sulcus length and visual hallucinations in Parkinson's disease suggests a neurobiological predisposition. Sci. Rep. 15 (1 15), 23123. https://doi.org/10.1038/s41598-025-04513-3, 2025.

Kostić, D., 2018. Mechanistic and topological explanations: an introduction. Synthese 195. https://doi.org/10.1007/s11229-016-1257-z.

Lanciego, J.L., Luquin, N., Obeso, J.A., 2012. Functional neuroanatomy of the basal ganglia. Cold Spring Harb. Perspect. Med. 2, a009621. https://doi.org/10.1101/cshperspect.a009621 a009621.

Li, J., Liao, H., Wang, T., Zi, Y., Zhang, L., Wang, M., Mao, Z., Song, C., Zhou, F., Shen, Q., Cai, S., Tan, C., 2021. Alterations of regional homogeneity in the mild and moderate stages of parkinson's disease. Front. Aging Neurosci. 13. https://doi.org/10.3389/fnagi.2021.676899.

Li, K., Su, W., Li, S.H., Jin, Y., Chen, H.B., 2018. Resting State fMRI: a Valuable Tool for Studying Cognitive Dysfunction in PD. Parkinsons Dis. https://doi.org/10.1155/2018/6278649.

Luo, C., Song, W., Chen, Q., Zheng, Z., Chen, K., Cao, B., Yang, J., Li, J., Huang, X., Gong, Q., Shang, H.-F., 2014. Reduced functional connectivity in early-stage drug-naive Parkinson's disease: a resting-state fMRI study. Neurobiol. Aging 35, 431–441. https://doi.org/10.1016/j.neurobiolaging.2013.08.018.

Makris, N., Liang, L., Biederman, J., Valera, E.M., Brown, A.B., Petty, C., Spencer, T.J., Faraone, S.V., Seidman, L.J., 2015. Toward defining the neural substrates of ADHD: a controlled structural MRI study in medication-naïve adults. J. Atten. Disord. 19, 944–953. https://doi.org/10.1177/1087054713506041.

Minosse, S., Garaci, F., Martino, F., Di Mauro, R., Melis, M., Di Giuliano, F., Picchi, E., Guerrisi, M., Floris, R., Di Girolamo, S., Di Girolamo, S., Toschi, N., 2021. Global and local brain connectivity changes associated with sudden unilateral sensorineural hearing loss. NMR Biomed. 34. https://doi.org/10.1002/nbm.4544.

Minosse, S., Garaci, F., Martino, F., Mauro, R.D.I., Melis, M., Giuliano, F.D.I., Picchi, E., Floris, R., Guerrisi, M., Girolamo, S.D.I., Toschi, N., 2020. Global and local reorganization of brain network connectivity in sudden sensorineural hearing loss. In: Proceedings of the Annual International Conference of the IEEE Engineering in Medicine and Biology Society. EMBS. https://doi.org/10.1109/EMBC44109.2020.9175688.

Minosse, S., Garaci, F., Martucci, A., Lanzafame, S., Di Giuliano, F., Picchi, E., Cesareo, M., Mancino, R., Guerrisi, M., Floris, R., Nucci, C., Toschi, N., 2019a. Disruption of brain network organization in primary open angle glaucoma. https://doi.org/10.1109/embc.2019.8857290.

Minosse, S., Garaci, F., Martucci, A., Lanzafame, S., Giuliano, F. Di, Picchi, E., Cesareo, M., Mancino, R., Guerrisi, M., Pistolese, C.A., Floris, R., Nucci, C., Toschi, N., 2019b. Primary open angle glaucoma is associated with functional brain network reorganization. Front. Neurol. 10. https://doi.org/10.3389/fneur.2019.01134.

Minosse, Silvia, Picchi, E., Giuliano, F. Di, Di Cio, F., Pistolese, C.A., Sarmati, L., Teti, E., Andreoni, M., Floris, R., Guerrisi, M., Garaci, F., Toschi, N., 2021a. Compartmental models for diffusion weighted MRI reveal widespread brain changes in HIV-infected patients. In: Proceedings of the Annual International Conference of the IEEE Engineering in Medicine and Biology Society. EMBS. https://doi.org/10.1109/EMBC46164.2021.9629510.

Minosse, Silvia, Picchi, E., Giuliano, F. Di, Teti, E., Sarmati, L., Pistolese, C.A., Lanzafame, S., Ciò, F. Di, Floris, R., Toschi, N., Guerrisi, M., Andreoni, M., Garaci, F., 2021b. Functional brain network reorganization in HIV infection. J. Neuroimaging 1–13. https://doi.org/10.1111/jon.12861.

Mirdamadi, J.L., 2016. Cerebellar role in Parkinson's disease. J. Neurophysiol. 116, 917–919. https://doi.org/10.1152/jn.01132.2015.

Moustafa, A.A., McMullan, R.D., Rostron, B., Hewedi, D.H., Haladjian, H.H., 2017. The thalamus as a relay station and gatekeeper: relevance to brain disorders. Rev. Neurosci. 28, 203–218. https://doi.org/10.1515/REVNEURO-2016-0067.

Newman, M., 2010. Networks: an introduction. Networks: An Introduction. https://doi.org/10.1093/acprof:oso/9780199206650.001.0001.

Newman, M.E.J., 2002. Assortative mixing in networks. Phys. Rev. Lett. https://doi.org/10.1103/PhysRevLett.89.208701.

O'Malley, K.L., 2010. The role of axonopathy in parkinson's disease. Exp Neurobiol 19. https://doi.org/10.5607/en.2010.19.3.115.

Onoda, K., Yamaguchi, S., 2015. Dissociative contributions of the anterior cingulate cortex to apathy and depression: topological evidence from resting-state functional MRI. Neuropsychologia 77, 10–18. https://doi.org/10.1016/j.neuropsychologia.2015.07.030.

Owens-Walton, C., Jakabek, D., Power, B.D., Walterfang, M., Velakoulis, D., van Westen, D., Looi, J.C.L., Shaw, M., Hansson, O., 2019. Increased functional connectivity of thalamic subdivisions in patients with Parkinson's disease. PLOS ONE 14 (9), e0222002. https://doi.org/10.1371/journal.pone.0222002.

Pfeiffer, H.C.V., Løkkegaard, A., Zoetmulder, M., Friberg, L., Werdelin, L., 2014. Cognitive impairment in early-stage non-demented Parkinson's disease patients. Acta Neurol. Scand. 129, 307–318. https://doi.org/10.1111/ANE.12189.

Piramide, N., De Micco, R., Siciliano, M., Silvestro, M., Tessitore, A., 2024. Resting-state functional MRI approaches to parkinsonisms and related dementia. Curr. Neurol. Neurosci. Rep. 24, 461–477. https://doi.org/10.1007/S11910-024-01365-8.

Planetta, P.J., Schulze, E.T., Geary, E.K., Corcos, D.M., Goldman, J.G., Little, D.M., Vaillancourt, D.E., 2013. Thalamic Projection Fiber Integrity in de novo Parkinson Disease. AJNR Am J Neuroradiol 34 (1), 74–79. https://doi.org/10.3174/ajnr.A3178.

Poewe, W., Seppi, K., Tanner, C., Halliday, G.M., Brundin, P., Volkmann, J., Schrag, A.E., Lang, A.E., 2017. PARKINSON DISEASE. Nature reviews disease primers. Nat. Rev. Dis. Primers 3.

Postuma, R.B., Berg, D., Stern, M., Poewe, W., Olanow, C.W., Oertel, W., Obeso, J., Marek, K., Litvan, I., Lang, A.E., Halliday, G., Goetz, C.G., Gasser, T., Dubois, B., Chan, P., Bloem, B.R., Adler, C.H., Deuschl, G., 2015. MDS clinical diagnostic criteria for Parkinson's disease. Mov. Disord. https://doi.org/10.1002/mds.26424.

Prodoehl, J., Burciu, R.G., Vaillancourt, D.E., 2014. Resting state functional magnetic resonance imaging in Parkinson's disease. Curr. Neurol. Neurosci. Rep. https://doi.org/10.1007/s11910-014-0448-6.

Reichardt, J., Bornholdt, S., 2006. Statistical mechanics of community detection. Phys. Rev. E - Stat. Nonlinear Soft Matter Phys. 74. https://doi.org/10.1103/PhysRevE.74.016110.

Rolls, E.T., Joliot, M., Tzourio-Mazoyer, N., 2015. Implementation of a new parcellation of the orbitofrontal cortex in the automated anatomical labeling atlas. Neuroimage 122. https://doi.org/10.1016/j.neuroimage.2015.07.075.

Rubinov, M., Sporns, O., 2010. Complex network measures of brain connectivity: uses and interpretations. Neuroimage. https://doi.org/10.1016/j.neuroimage.2009.10.003.

Rudebeck, P.H., Rich, E.L., 2018. Orbitofrontal cortex. Curr. Biol. 28, R1083–R1088. https://doi.org/10.1016/j.cub.2018.07.018.

Sang, L., Zhang, Jiuquan, Wang, L., Zhang, Jingna, Zhang, Y., Li, P., Wang, J., Qiu, M., 2015. Alteration of brain functional networks in early-stage parkinson's disease: a resting-state fMRI study. PLoS One 10, e0141815. https://doi.org/10.1371/journal.pone.0141815.

Skidmore, F., Korenkevych, D., Liu, Y., He, G., Bullmore, E., Pardalos, P.M., 2011. Connectivity brain networks based on wavelet correlation analysis in Parkinson fMRI data. Neurosci. Lett. 499. https://doi.org/10.1016/j.neulet.2011.05.030.

Tagliaferro, P., Kareva, T., Oo, T.F., Yarygina, O., Kholodilov, N., Burke, R.E., 2015. An early axonopathy in a hLRRK2(R1441G) transgenic model of Parkinson disease. Neurobiol. Dis. 82. https://doi.org/10.1016/j.nbd.2015.07.009.

Tahmasian, M., Bettray, L.M., van Eimeren, T., Drzezga, A., Timmermann, L., Eickhoff, C. R., Eickhoff, S.B., Eggers, C., 2015. A systematic review on the applications of resting-state fMRI in Parkinson's disease: does dopamine replacement therapy play a role? Cortex. https://doi.org/10.1016/j.cortex.2015.08.005.

Vo, A., Sako, W., Fujita, K., Peng, S., Mattis, P.J., Skidmore, F.M., Ma, Y., Uluğ, A.M., Eidelberg, D., 2017. Parkinson's disease-related network topographies characterized with resting state functional MRI. Hum. Brain Mapp. 38. https://doi.org/10.1002/hbm.23260.

Wang, K., Chen, Y., Chai, W., Liu, C., Tan, L., He, J., Liu, X., Wang, G., Zhang, M., Long, L., Xiao, B., Xie, F., Song, Y., 2025. Abnormal functional connectivity of paracingulate gyrus in patients with temporal lobe epilepsy-comorbid sleep disorders. Epilepsy Behav. 168, 110408. https://doi.org/10.1016/J.YEBEH.2025.110408.

Zhang, C., Dou, B., Wang, J., Xu, K., Zhang, H., Sami, M.U., Hu, C., Rong, Y., Xiao, Q., Chen, N., Li, K., 2019. Dynamic alterations of spontaneous neural activity in parkinson's disease: a resting-state fMRI study. Front. Neurol. 10. https://doi.org/10.3389/fneur.2019.01052.

Zhou, F., Tan, C., Song, C., Wang, M., Yuan, J., Liu, Y., Cai, S., Liu, Q., Shen, Q., Tang, Y., Li, X., Liao, H., 2023. Abnormal intra- and inter-network functional connectivity of brain networks in early-onset Parkinson's disease and late-onset Parkinson's disease. Front. Aging Neurosci. 15. https://doi.org/10.3389/fnagi.2023.1132723.